Dependence of the self-diffusion coefficient on the q-gap value in fluids

Konstantin P. Zhukov,[1] Nikita P. Kryuchkov[1]*and Stanislav O. Yurchenko[1]

[1]Bauman Moscow State Technical University, 2nd Baumanskaya Street 5, 105005 Moscow, Russia

Abstract

abstractabstractabstractabstractabstractabstractabstractabstractabstract abstractabstractabstractabstractabstractabstractabstractabstract abstractabstractabstractabstractabstractabstractabstractabstract abstractabstractabstractabstractabstractabstract abstractabstractabstractabstractabstractabstractabstract. abstractabstractabstractabstractabstractabstractabstract abstractabstractabstractabstractabstractabstractabstract

Introduction

The excitation spectra describe the propagation of mechanical waves in medium and make it possible to determine the energy distribution in the phonon system at various frequencies and wave vectors. These spectra arise from correlated many-body dynamics and manifest as distinct branches in dispersion relations – longitudinal acoustic modes governing density fluctuations and transverse modes reflecting shear resistance. The analysis of collective excitation spectra offers valuable insights into various phenomena and associated properties, such as elastic, thermodynamic, and transport characteristics in crystals, condensed matter, and strongly coupled plasmas.[1–3].

Despite considerable progress in understanding collective excitations in crystalline structures using lattice dynamics theory, applying these frameworks to disordered systems (e.g., liquids and amorphous materials) faces major theoretical difficulties. Unlike crystalline solids, liquids are characterized by the absence of small parameter related to anharmonicity[4]. Hence, traditional analytical approaches based on the assumption of small atomic fluctuations about fixed equilibrium positions are inapplicable. In recent studies, collective excitations have gained significant attention in the context of fluid thermodynamics and collective dynamics.[4–19]. One of the distinct features of excitation spectra in fluids is the q-gap – a discontinuity in transverse excitation dispersion curves arising from their instability at long wavelengths. This specific property characterizes the ability to maintain the propagation of transverse waves in liquids which is for significant importance for various applied industries, including biotechnology, chemical physics, and soft materials.

The definition of q-gap was first formulated within the framework of Maxwell-Frenkel approach[20] as $q_g = 1/2c\tau$, where c is the transverse sound velocity and τ is the Maxwell relaxation time. Originally identified in dusty plasmas[21], q-gap have since been extensively studied by molecular dynamics simulations of classical liquids[5, 7, 22–28] and other liquid systems[9, 29–31] and experiments in liquid metals and colloidal suspensions[31–35]. Additionally, the similarity between vibrational modes at high frequency/wave-vector in liquids and solids have been experimentally verified[36–40]. The recent paper[41] reviews the emergence of gapped momentum states across diverse physical systems, ranging from ordinary liquids to holographic models, discussing their origin, implications, and theoretical approaches. The review underscores the importance of q-gap in characterizing collective behavior across these systems, particularly in distinguishing between vibrational and diffusive regimes. Recent work[7] establishes a correlation between the q-gap width and the system's heat capacity, implying its potential influence on other thermodynamic properties, including the self-diffusion coefficient. However, this topic remains little studied.

In this work we establish a correlation between the self-diffusion coefficient D and the q-gap width in classical liquids through molecular dynamics simulations of Lennard-Jones, Yukawa, Embedded atom model (EAM for iron) and machine-learning-based (ML-IAP for liquid aluminum) potentials across 2D and 3D configurations. Analysis of velocity current spectra using two-oscillator model reveals a universal linear dependence of D on q-gap width across all investigated interaction potentials in 3D case. We demonstrate that 3D systems exhibit discontinuous growth of D during melting due to crystalline lattice breakdown and metastable cluster formation, while 2D systems show smooth transitions consistent with Kosterlitz-Thouless-Halperin-Nelson-Young (KTHNY) melting mediated by topological

*Corresponding author: kruchkov_nkt@mail.ru
Received: October 20, 2023, **Published:** December 14, 2023

defects. The observed temperature-dependent expansion of the q-gap and emergence of solid-like transverse modes for $q > q_g$ confirm its role as a critical parameter separating vibrational and diffusive regimes.

Methods

We considered systems of particles interacting via the Lennard-Jones (LJ) and Yukawa (Ykw) pair potentials:

$$\varphi_{\mathrm{LJ}}(r) = 4\varepsilon\left[\left(\frac{\sigma}{r}\right)^{12} - \left(\frac{\sigma}{r}\right)^{6}\right], \tag{1}$$

$$\varphi_{\mathrm{Ykw}}(r) = A\frac{e^{-k_D r}}{r}, \tag{2}$$

where ε and σ are the energy and length scale of the interaction, respectively; A and κ are scaling parameters which where chosen as $A = 1$, $k_D = \lambda_D^{-1} = 1$. Corresponding coupling and screening parameters are $\Gamma = A(ak_BT)^{-1}$ and $\kappa = a\lambda_D^{-1}$, respectively. Here λ_D is the Debye length, $a = (3/4\pi n)^{1/3}$ is the Wigner-Seitz radius, where $n = N/V$ is the numerical density, k_B is the Boltzmann constant and T is the temperature.

We have studied 3D and 2D fluids consisting of $N = 4000$ ($N = 4900$ in 2D case) particles in an NVT ensemble with a Nose–Hoover thermostat. The initial state of the system was a cubic lattice (a square in 2D case) with a size $L = 10$ ($L = 70$ in 2D case) with periodic boundary conditions with Maxwell distribution of velocities. The cutoff radius of interaction was chosen as $r_{\mathrm{cut}} = 7.5n^{-1/d}$, where $n = N/V$ is the numerical density and d is the space dimension. The mass m, length σ, and energy ε were normalized to unity.

The interatomic potential with machine learning (ML-IAP) for liquid aluminum[42] was also considered:

$$\varphi_{\text{ML-IAP}}(r) = \varphi_{\mathrm{ref}}(r) + \sum_{i=1}^{N} E^i_{\mathrm{SNAP}}, \tag{3}$$

where E_{ref} denotes a reference potential and E^i_{SNAP} is the total energy of atom i relative to the atoms in its neighborhood, governed by the spectral neighbor analysis potential method (SNAP)[43]. Ziegler-Biersack-Littmark (ZBL) potential[44] is used as a reference potential. The SNAP energy for each atom is calculated using a linear combination of the bispectrum components $\mathbf{B}^i$

$$E^i_{\mathrm{SNAP}} = \boldsymbol{\beta} \times \mathbf{B}^i, \tag{4}$$

where $\boldsymbol{\beta}$ are linear coefficients and $\mathbf{B}^i$ are descriptors of the local environment of atom i. Obtained using machine learning coefficients[45] $\boldsymbol{\beta}$ were used in this work.

Simulations of liquid Al were performed in a three-dimensional face-centered cubic box with dimensions of $Lx = Ly = Lz = 10a$, where a is lattice constant, with mass density $\rho = 2.7\mathrm{g/cm}^3$. The remaining simulation details including number of particles, thermostating and boundary conditions follow previously established setup.

Moreover, we considered liquid iron using Embedded atom model (EAM). The general form of this potential can be expressed as:

$$E_i = \sum_i F(\rho_i) + \frac{1}{2}\sum_i \sum_{j\neq i} \varphi_{\mathrm{p}}(r_{ij}), \tag{5}$$

where $F_i(\rho_i)$ denotes the embedding energy for atom i, a function of the local electron density ρ_i. This local density is computed as a superposition of the contributions from all neighboring atoms j:

$$\rho_i = \sum_{j\neq i} \rho(r_{ij}). \tag{6}$$

In these expressions, $\varphi_{\mathrm{p}}(r_{ij})$ represents the pairwise potential between atoms i and j, separated by a distance r_{ij}. The specific functional forms for $F(\rho)$, $\rho(r)$, and $\varphi_{\mathrm{p}}(r)$ employed in this work are those established in the corresponding paper[46].

The mass density $\rho = 10g/cm^3$ was used in the simulations for liquid iron. The remaining simulation parameters correspond to those employed for liquid iron.

Simulations of fluids of particles interacting via the Lennard-Jones and Yukawa potentials were performed using the numerical time step $\Delta t = 5 \times 10^{-3}\sqrt{m\sigma^2/\varepsilon}$. For ML-IAP and EAM potentials in liquid aluminum and iron the time step $\Delta t = 5$ fs was chosen. All simulations where performed with the LAMMPS package[47] for 5×10^4 time steps, where the first 5000 were used for system relaxation.

Fluids in states near the freezing line were considered. Chosen parameters for each system are represented in Table 1. The Lennard-Jones units are used for LJ and Yukawa systems throughout the paper.

To obtain excitation spectra of the fluids, we studied the velocity current spectra[48]

$$C_{L,T}(\mathbf{q},\omega) = \int dt\, e^{i\omega t}\, \mathrm{Re}\langle j_{L,T}(\mathbf{q},t) j_{L,T}(-\mathbf{q},0)\rangle, \tag{7}$$

where $\mathbf{j}(\mathbf{q},t) = N^{-1}\sum_s^N \mathbf{v}_s(t)\exp(i\mathbf{q}\mathbf{r}_s(t))$ is the velocity current; $\mathbf{v}_s(t) = \dot{\mathbf{r}}_s(t)$ is the velocity of particle s; $\mathbf{j}_L = \mathbf{q}(\mathbf{j}\cdot\mathbf{q})/q^2$ and $\mathbf{j}_T = (\mathbf{j}\cdot\mathbf{e}_\perp)\mathbf{e}_\perp$ are longitudinal and transverse components of velocity current, respectively (here $\mathbf{e}_\perp$ is unit vector, normal to the $\mathbf{q}$) and the brackets $\langle \ldots \rangle$ denote ensemble average.

Table 1: *Chosen states of considered systems.*

Potential	Dimension	Density	Temperature
ML-IAP (Al)	3D	2.7 g/cm^3	1560 — 2560 K
LJ	3D	1.00	1.6 — 7.0
		1.10	2.7 — 8.0
		1.20	4.0 — 9.0
		1.30	5.8 — 15.6
		1.40	8.1 — 17.9
		1.60	14.6 — 21.8
		1.80	24.2 — 29.8
		2.00	37.4 – 44.8
	2D	0.80	0.60 — 3.10
		0.85	1.00 — 3.50
		0.90	2.00 — 4.50
		κ	Γ
Yukawa	3D	1.00	217 — 117
		1.25	250 — 110
		1.50	270 — 86
		2.00	440 — 157
		2.50	750 — 305
		3.00	1185 — 665
	2D	1.00	177 — 77
		1.50	250 — 73
		2.00	395 — 112
		2.50	681 — 285
		3.00	1120 — 800

The isotropy of simple fluids allows us to average $C_{L,T}(\mathbf{q},\omega)$ across all wavevector $\mathbf{q}$ directions:

$$C_{L,T}(q,\omega) = \frac{1}{N_q}\sum_{|\mathbf{q}|=q}^{N_q} C_{L,T}(\mathbf{q},\omega), \tag{8}$$

where N_q is the number of directions used for averaging.

Further, to obtain transverse dispersion relations $\omega_{L,T}(q)$ the values of $C_{L,T}(q,\omega)$ were investigated by single mode analysis

$$\begin{aligned} C_{L,T}(q,\omega) \;\propto\; & \frac{\Gamma_{L,T}(q)}{(\omega-\omega_{L,T}(q))^2+\Gamma_{L,T}^2(q)} \\ & + \frac{\Gamma_{L,T}(q)}{(\omega+\omega_{L,T}(q))^2+\Gamma_{L,T}^2(q)} \end{aligned} \tag{9}$$

and two-oscillator model[5]

$$\begin{aligned} C(q,\omega) \;\propto\; & \frac{\Gamma_L}{(\omega-\omega_L)^2+\Gamma_L^2} + \frac{\Gamma_L}{(\omega+\omega_L)^2+\Gamma_L^2} \\ & + \frac{(d-1)\Gamma_T}{(\omega-\omega_T)^2+\Gamma_T^2} + \frac{(d-1)\Gamma_T}{(\omega+\omega_T)^2+\Gamma_T^2}, \end{aligned} \tag{10}$$

where d is the space dimension.

The self-diffusion coefficient D was calculated using mean-square deviation of particles:

$$\mathrm{MSD}(t) = N^{-1}\sum_{s}^{N}(\mathbf{r}_s(t)-\mathbf{r}_s(0))^2, \tag{11}$$

$$D = \lim_{t\to\infty}\frac{\mathrm{MSD}(t)}{2dt}, \tag{12}$$

where d, as clarified earlier, is the space dimension.

Results

The fluids were studied at the same densities (κ for Al), but under different temperatures (Γ for Al).

To the obtain excitation spectra, velocity current spectra was calculated in a certain range of wavenumber values. Velocity current spectra for considered systems are presented in supplementary material.

To obtain q-gap values, dispersion relations $\omega_{L,T}(q)$ using fits by Eqs. (9) and (10) were calculated. Low-frequency terms $\omega_T(q)$ for 3D Lennard-Jones fluid at $T = 5$, 6 and 7 are demonstrated in Fig. 1. Blue and red solid lines on the plots show results obtained using the single-mode analysis (9) and the two-oscillator model (10), respectively. For both approximation models, a clear q-gap region with zero ω_T values is observed, confirming the applicability of model (10) for identifying gap states in dispersion relations. Note that q-gap values calculated using models (9) and (10) show minor differences at low

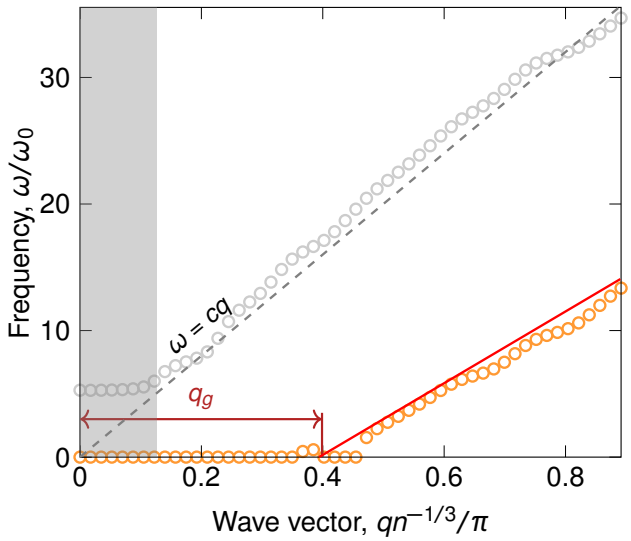

Figure 1: *Dispersion relations $\omega_{L,T}(q)$ for a 3D Lennard-Jones fluid at density $n = 1$ and temperature $T = 5$. Transverse (ω_T) and longitudinal (ω_L) modes are represented by orange and gray circles, respectively. The gray and red lines depict the theoretical asymptotic curves $\omega = cq$. The dark gray zone indicates the region where $qn^{-1/3} < 2\pi/L$ and finite-size effects are significant (L being the system size).*

temperatures but exhibit increasing divergence with rising temperature, consistent with data from recent study[5]. Additionally, an increase in q-gap width with increasing temperature is observed, which also aligns with results from [7]. Similar dispersion relations for other systems are presented in supplementary material.

The dependencies of the self-diffusion coefficient, calculated using particle MSD given by Eq. (12), on the q-gap width for the considered systems are shown in Figures 3, 4, and 5 for both three- and two-dimensional cases.

The plots display values corresponding to the q-gap obtained from both single-mode analysis (blue circles) and the two-oscillator model (red diamonds), along with their linear approximations. A clear linear relationship between the coefficient D and the q-gap width is observed for both three- and two-dimensional cases. Notably, for three-dimensional systems, the dependence does not pass through the origin, which corresponds to a crystalline state with zero values of D and q-gap. Thus, the obtained dependencies indicate a nonlinear growth of the self-diffusion coefficient D with increasing q-gap in three-dimensional classical fluids during melting. However, in this work, we were unable to analyze systems with $q_g < q_{g,\min}$ (values of $q_{g,\min}$ are given in Table 2), so clarifying the behavior of $D(q_g)$ in the melting region requires further investigation. A systematic discrepancy between the data from single-mode analysis and the two-oscillator model was also observed: the linearized dependencies show differences in slope angles, the nature of which requires separate study.

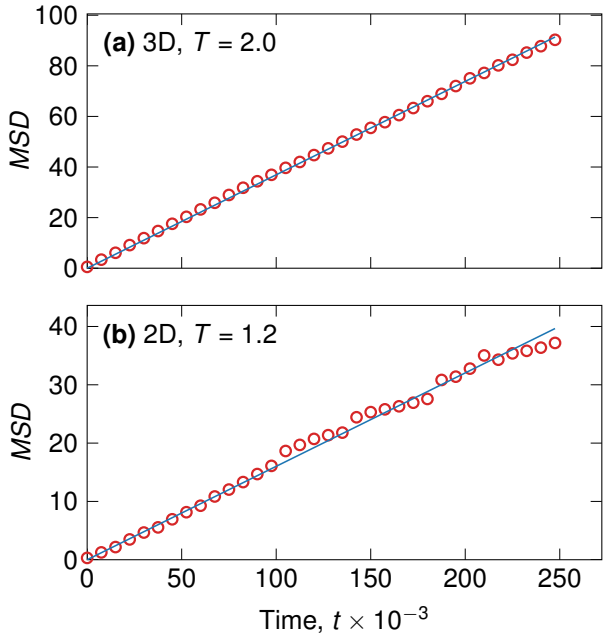

Figure 2: *Dependence of the MSD on the time t for the Lennard-Jones potential in three- and two-dimensional cases.*

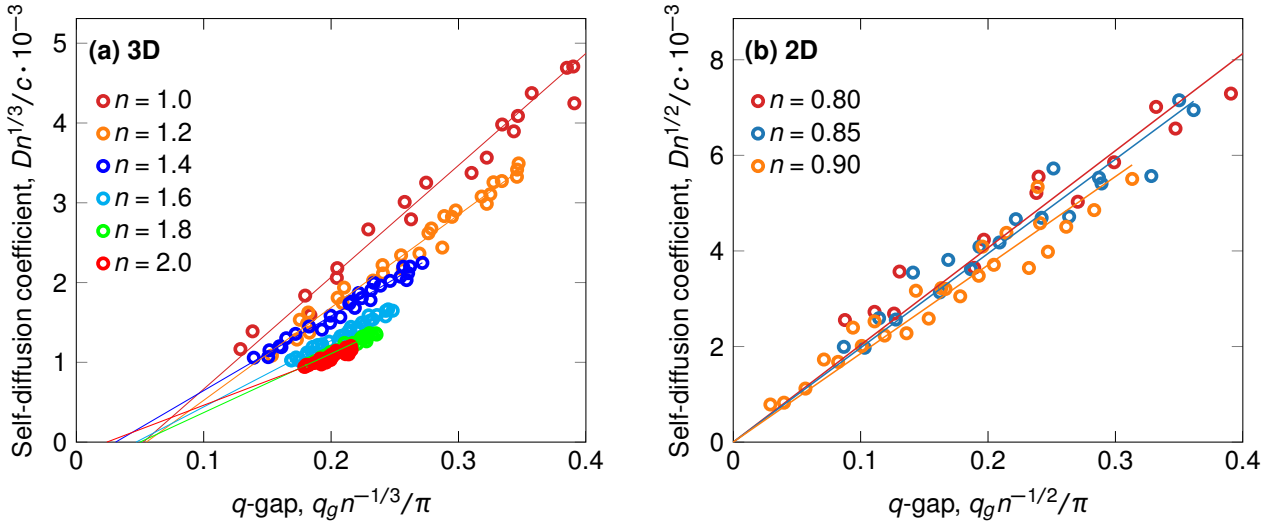

Figure 3: *Dependence of the self-diffusion coefficient D on the q-gap width for the Lennard-Jones fluid in (**a**) 3D and (**b**) 2D cases. (**a**) Results for 3D systems with densities n = 1 — 2. Dashed colored lines are linear approximations. The scaled area is provided to clarify parameter variations at the melting point. (**b**) Results for 2D systems with densities n = 0.8 — 0.9. Solid colored lines are piecewise linear approximations.*

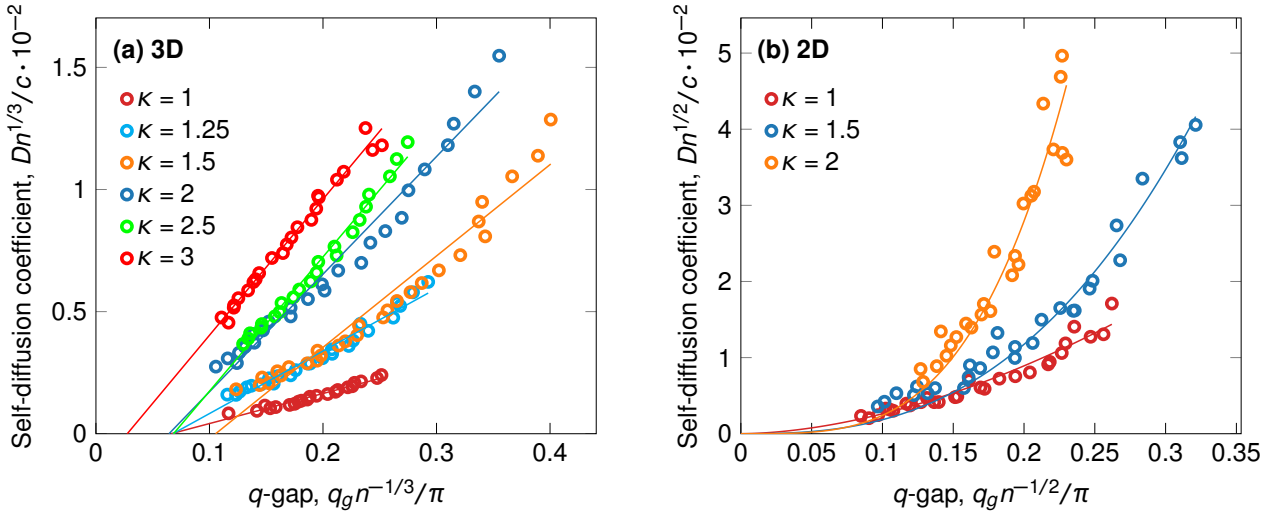

Figure 4: *Dependence of the self-diffusion coefficient D on the q-gap width for the Yukawa fluid in (**a**) 3D and (**b**) 2D cases. (**a**) Results for 3D systems screening parameters κ = 1 — 3. Solid colored lines are linear approximations. (**b**) Results for 2D systems with screening parameters κ = 1 — 3.*

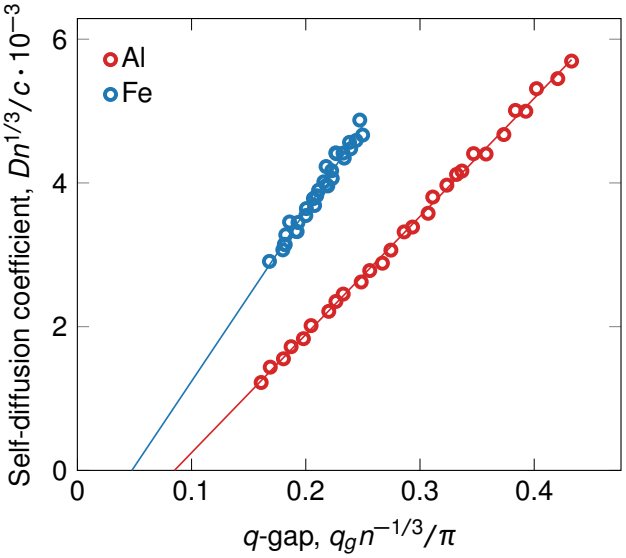

Figure 5: *Dependence of the self-diffusion coefficient D on the q-gap width for 3D liquid aluminum at density $\rho = 2.7$ g/cm^3.*

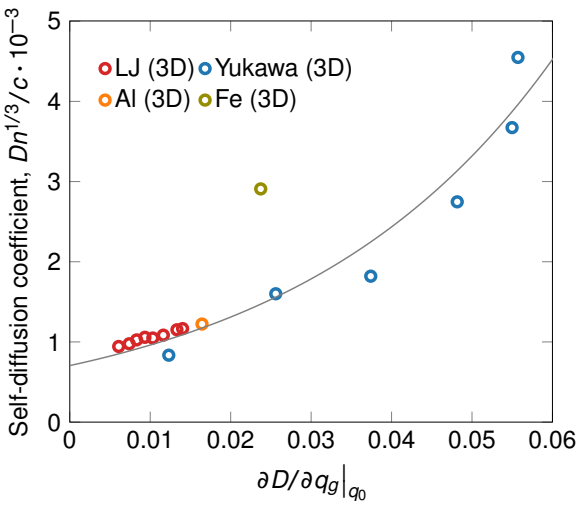

Figure 6: *Scatter plot with colormap of $D(q_g)$ values near the melting point: the color of each point represents the slope value k of the corresponding dependence.*

On the other hand, this effect is not observed in two-dimensional systems, and the least-squares approximations intersect the abscissa axis near the origin. This distinction, as we assume, appears from fundamental differences in the melting scenarios of 2D and 3D systems. In three-dimensional systems, first-order phase transitions dominate, characterized by jumps in thermodynamic parameters and density inhomogeneities, whereas in two-dimensional systems, the Kosterlitz-Thouless-Halperin-Nelson-Young (KTHNY) theory of two-dimensional melting is applied, involving the formation of topological defects and suppression of long-range order[49]. These differences are caused by the enhanced role of thermal fluctuations at $d < 3$ and the constraints imposed by the Mermin-Wagner theorem[50], which prohibits spontaneous symmetry breaking in two-dimensional systems. However, a detailed study of this phenomenon remains a subject for future work.

Discussion

References

1. March, Norman H., Tosi, Mario P., and Tosi, Mario P. *Introduction to liquid state physics*. eng. River Edge, NJ: World Scientific, 2002. ISBN: 978-981-02-4652-5, 978-981-02-4639-6.

2. Dove, Martin T. *Introduction to Lattice Dynamics*. 1st ed. Cambridge University Press, Oct. 1993. ISBN: 978-0-521-39293-8, 978-0-521-39894-7, 978-0-511-61988-5. DOI: 10.1017/cbo9780511619885. URL: https://www.cambridge.org/core/product/identifier/

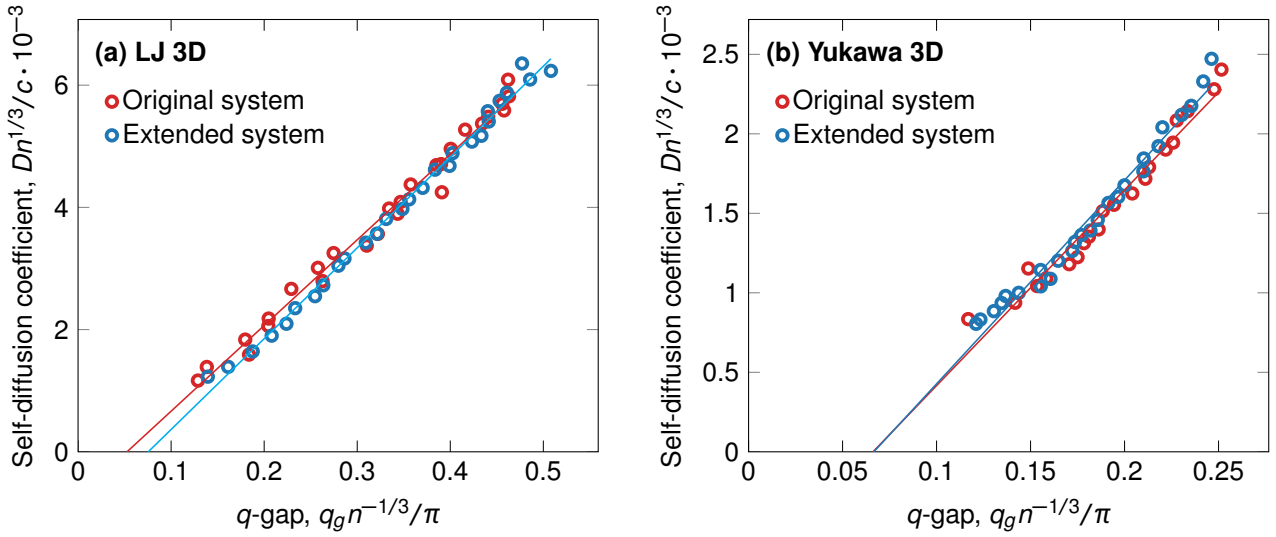

Figure 7: *Scatter plot with colormap of $D(q_g)$ values near the melting point: the color of each point represents the slope value k of the corresponding dependence.*

Table 2: *Minimum values of q_g and corresponding slopes for studied systems*

Potential	Dimension	Density	Value of q_g near the MP, q_0	$\left(\frac{dD}{dq_g}\right)_{q_0}$
ML-IAP (Al)	3D	2.7 g/cm^3	0.078	0.0130
LJ	3D	1.0	0.165	0.0166
		1.1	0.159	0.0142
		1.2	0.157	0.0136
		1.3	0.151	0.0124
		1.4	0.151	0.0110
		1.6	0.169	0.0079
		1.8	0.182	0.0074
		2.0	0.170	0.0062
	2D	0.80	0.172	0.039
		0.85	0.119	0.034
		0.90	0.056	0.029
Yukawa		κ		
	3D	1.00	0.115	0.015
		1.25	0.105	0.027
		1.50	0.123	0.042
		2.00	0.106	0.052
		2.50	0.130	0.058
		3.00	0.111	0.098
	2D	1.00	0.045	
		1.50	0.048	
		2.00	0.048	
		2.50	0.048	
		3.00	0.042	

9780511619885 / type / book (visited on 07/15/2025).

3. Ziman, J. M. *Electrons and phonons: the theory of transport phenomena in solids*. Oxford classic texts in the physical sciences. Oxford : New York: Clarendon Press ; Oxford University Press, 2001. ISBN: 978-0-19-850779-6.
4. Trachenko, K and Brazhkin, V V. Collective modes and thermodynamics of the liquid state. en. In: Reports on Progress in Physics 79.1 (Dec. 2015). Publisher: IOP Publishing, p. 016502. ISSN: 0034-4885. DOI: 10.1088/0034-4885/79/1/016502. URL: https://dx.doi.org/10.1088/0034-4885/79/1/016502 (visited on 03/02/2025).
5. Kryuchkov, Nikita P et al. Excitation spectra in fluids: How to analyze them properly. In: Scientific reports 9.1 (2019). Publisher: Nature Publishing Group UK London, p. 10483. DOI: 10.1038/s41598-019-46979-y.
6. Yakovlev, Egor V et al. Direct experimental evidence of longitudinal and transverse mode hybridization and anticrossing in simple model fluids. In: The Journal of Physical Chemistry Letters 11.4 (2020). Publisher: ACS Publications, pp. 1370–1376. DOI: 10.1021/acs.jpclett.9b03568.s001.
7. Kryuchkov, Nikita P. et al. Universal Effect of Excitation Dispersion on the Heat Capacity and Gapped States in Fluids. en. In: Physical Review Letters 125.12 (Sept. 2020), p. 125501. ISSN: 0031-9007, 1079-7114. DOI: 10.1103/PhysRevLett.125.125501. URL: https://link.aps.org/doi/10.1103/PhysRevLett.125.125501 (visited on 03/10/2025).
8. Khrapak, Sergey A. Vibrational model of thermal conduction for fluids with soft interactions. In: Physical Review E 103.1 (Jan. 2021). Publisher: American Physical Society, p. 013207. DOI: 10.1103/PhysRevE.103.013207. URL: https://link.aps.org/doi/10.1103/PhysRevE.103.013207 (visited on 03/02/2025).
9. Kryuchkov, Nikita P and Yurchenko, Stanislav O. Collective excitations in active fluids: Microflows and breakdown in spectral equipartition of kinetic energy. In: The Journal of Chemical Physics 155.2 (2021). Publisher: AIP Publishing. DOI: 10.1063/5.0054854.
10. Stamper, Caleb et al. Experimental Confirmation of the Universal Law for the Vibrational Density of States of Liquids. en. In: The Journal of Physical Chemistry Letters 13.13 (Apr. 2022), pp. 3105–3111. ISSN: 1948-7185, 1948-7185. DOI: 10.1021/acs.jpclett.2c00297. URL: https://pubs.acs.org/doi/10.1021/acs.jpclett.2c00297 (visited on 03/08/2025).
11. Hofmann, Johannes and Das Sarma, Sankar. Collective modes in interacting two-dimensional tomographic Fermi liquids. In: Physical Review B 106.20 (Nov. 2022). Publisher: American Physical Society, p. 205412. DOI: 10.1103/PhysRevB.106.205412. URL: https://link.aps.org/doi/10.1103/PhysRevB.106.205412 (visited on 03/02/2025).
12. Zhao, Andrew Z. and Garay, Javier E. High temperature liquid thermal conductivity: A review of measurement techniques, theoretical understanding, and energy applications. en. In: Progress in Materials Science 139 (Oct. 2023), p. 101180. ISSN: 00796425. DOI: 10.1016/j.pmatsci.2023.101180. URL: https://linkinghub.elsevier.com/retrieve/pii/S0079642523001123 (visited on 03/08/2025).
13. Huang, Dong et al. Revealing the supercritical dynamics of dusty plasmas and their liquidlike to gaslike dynamical crossover. en. In: Physical Review Research 5.1 (Feb. 2023), p. 013149. ISSN: 2643-1564. DOI: 10.1103/PhysRevResearch.5.013149. URL: https://link.aps.org/doi/10.1103/PhysRevResearch.5.013149 (visited on 03/08/2025).
14. Cockrell, Cillian and Dragović, Aleksandra. Thermodynamics and collective modes in hydrogen-bonded fluids. In: The Journal of Chemical Physics 160.11 (2024). Publisher: AIP Publishing. DOI: 10.1063/5.0201689.
15. Khrapak, S. A. Elementary vibrational model for transport properties of dense fluids. In: Physics Reports. Elementary vibrational model for transport properties of dense fluids 1050 (Jan. 2024), pp. 1–29. ISSN: 0370-1573. DOI: 10.1016/j.physrep.2023.11.004. URL: https://www.sciencedirect.com/science/article/pii/S0370157323003885 (visited on 03/08/2025).
16. Yu, Nichen et al. Universal scaling of transverse sound speed and its isomorphic property in Yukawa fluids. In: Physical Review E 109.3 (2024). Publisher: APS, p. 035202. DOI: 10.1103/physreve.109.035202.
17. Khrapak, S. A. Entropy of strongly coupled Yukawa fluids. en. In: Physical Review E 110.3 (Sept. 2024), p. 034602. ISSN: 2470-0045, 2470-0053. DOI: 10.1103/PhysRevE.110.034602. URL: https://link.aps.org/doi/10.

1103/PhysRevE.110.034602 (visited on 03/08/2025).

18. Cockrell, Cillian et al. Thermodynamics and transport in molten chloride salts and their mixtures. In: Physical Chemistry Chemical Physics 27.3 (2025). Publisher: Royal Society of Chemistry, pp. 1604–1615. DOI: 10.1039/d4cp04180a.
19. Huang, Dong et al. Fundamental Origin of Viscosity in 2D Simple Liquids. In: arXiv preprint arXiv:2502.12522 (2025). DOI: 10.1063/5.0266423.
20. Frenkel, J. *Kinetic Theory Of Liquids*. eng. 1946. URL: http://archive.org/details/in.ernet.dli.2015.53485 (visited on 03/07/2025).
21. Nosenko, V, Goree, J, and Piel, A. Cutoff wave number for shear waves in a two-dimensional Yukawa system (dusty plasma). In: Physical review letters 97.11 (2006). Publisher: APS, p. 115001. DOI: 10.1103/physrevlett.97.115001.
22. Yang, C. et al. Emergence and Evolution of the k Gap in Spectra of Liquid and Supercritical States. en. In: Physical Review Letters 118.21 (May 2017), p. 215502. ISSN: 0031-9007, 1079-7114. DOI: 10.1103/PhysRevLett.118.215502. URL: http://link.aps.org/doi/10.1103/PhysRevLett.118.215502 (visited on 03/08/2025).
23. Guarini, Eleonora et al. Onset of collective excitations in the transverse dynamics of simple fluids. In: Physical Review E 107.1 (2023). Publisher: APS, p. 014139. DOI: 10.1103/physreve.107.014139.
24. Fomin, Yu D. Dispersion of acoustic excitations in tetrahedral liquids. In: Journal of Physics: Condensed Matter 32.39 (2020). Publisher: IOP Publishing, p. 395101. DOI: 10.1088/1361-648x/ab962e.
25. Toledo-Marín, J Quetzalcóatl and Naumis, Gerardo G. Viscoelasticity and dynamical gaps: rigidity in crystallization and glass-forming liquids. In: Journal of Non-Crystalline Solids: X 3 (2019). Publisher: Elsevier, p. 100030. DOI: 10.1016/j.nocx.2019.100030.
26. Khrapak, Sergey A et al. Collective modes of two-dimensional classical Coulomb fluids. In: The Journal of Chemical Physics 149.13 (2018). Publisher: AIP Publishing. DOI: 10.1063/1.5050708.
27. Bryk, Taras, Kopcha, Maria, and Yidak, Ihor. Propagation gap for shear waves in binary liquids: Analytical and simulation study. In: The Journal of Chemical Physics 161.18 (2024). Publisher: AIP Publishing. DOI: 10.1063/5.0236047.
28. Bryk, Taras et al. Non-hydrodynamic transverse collective excitations in hard-sphere fluids. In: The Journal of Chemical Physics 147.6 (2017). Publisher: AIP Publishing. DOI: 10.1063/1.4997640.
29. Khrapak, Sergey A et al. Onset of transverse (shear) waves in strongly-coupled Yukawa fluids. In: The Journal of chemical physics 150.10 (2019). Publisher: AIP Publishing. DOI: 10.1063/1.5088141.
30. Ge, Zhenyu et al. Observation of fast sound in two-dimensional dusty plasma liquids. In: Physical Review E 107.5 (2023). Publisher: APS, p. 055211. DOI: 10.1103/physreve.107.055211.
31. Khusnutdinoff, R. M. et al. Collective modes and gapped momentum states in liquid Ga: Experiment, theory, and simulation. In: Physical Review B 101.21 (June 2020). Publisher: American Physical Society, p. 214312. DOI: 10.1103/PhysRevB.101.214312. URL: https://link.aps.org/doi/10.1103/PhysRevB.101.214312 (visited on 03/02/2025).
32. Hosokawa, S. et al. Transverse Acoustic Excitations in Liquid Ga. en. In: Physical Review Letters 102.10 (Mar. 2009), p. 105502. ISSN: 0031-9007, 1079-7114. DOI: 10.1103/PhysRevLett.102.105502. URL: https://link.aps.org/doi/10.1103/PhysRevLett.102.105502 (visited on 03/07/2025).
33. Hosokawa, S et al. Transverse excitations in liquid Sn. In: Journal of Physics: Condensed Matter 25.11 (Mar. 2013), p. 112101. ISSN: 0953-8984, 1361-648X. DOI: 10.1088/0953-8984/25/11/112101. URL: https://iopscience.iop.org/article/10.1088/0953-8984/25/11/112101 (visited on 03/07/2025).
34. Hosokawa, S et al. Transverse excitations in liquid Fe, Cu and Zn. In: Journal of Physics: Condensed Matter 27.19 (May 2015), p. 194104. ISSN: 0953-8984, 1361-648X. DOI: 10.1088/0953-8984/27/19/194104. URL: https://iopscience.iop.org/article/10.1088/0953-8984/27/19/194104 (visited on 03/07/2025).

35. Jiang, Cunyuan et al. Experimental observation of gapped shear waves and liquid-like to gas-like dynamical crossover in active granular matter. en. In: Communications Physics 8.1 (Feb. 2025). Publisher: Nature Publishing Group, pp. 1–12. ISSN: 2399-3650. DOI: 10.1038/s42005-025-02008-1. URL: https://www.nature.com/articles/s42005-025-02008-1 (visited on 03/02/2025).

36. Ruocco, G et al. Equivalence of the sound velocity in water and ice at mesoscopic wavelengths. In: Nature 379.6565 (1996). Publisher: Nature Publishing Group UK London, pp. 521–523. DOI: 10.1038/379521a0.

37. Giordano, Valentina M. and Monaco, Giulio. Fingerprints of order and disorder on the high-frequency dynamics of liquids. en. In: Proceedings of the National Academy of Sciences 107.51 (Dec. 2010), pp. 21985–21989. ISSN: 0027-8424, 1091-6490. DOI: 10.1073/pnas.1006319107. URL: https://pnas.org/doi/full/10.1073/pnas.1006319107 (visited on 03/07/2025).

38. Scopigno, Tullio, Ruocco, Giancarlo, and Sette, Francesco. Microscopic dynamics in liquid metals: The experimental point of view. In: Reviews of Modern Physics 77.3 (2005). Publisher: APS, pp. 881–933. DOI: 10.1103/revmodphys.77.881.

39. Noirez, Laurence and Baroni, Patrick. Identification of a low-frequency elastic behaviour in liquid water. In: Journal of Physics: Condensed Matter 24.37 (2012). Publisher: IOP Publishing, p. 372101. DOI: 10.1088/0953-8984/24/37/372101.

40. Yu, Yuanxi et al. Unveiling the solid-like dynamics of liquids at low-frequency via nano-confinement. In: arXiv preprint arXiv:2307.11429 (2023). DOI: 10.1063/1.1637145.

41. Baggioli, Matteo et al. Gapped momentum states. In: Physics Reports. Gapped momentum states 865 (June 2020), pp. 1–44. ISSN: 0370-1573. DOI: 10.1016/j.physrep.2020.04.002. URL: https://www.sciencedirect.com/science/article/pii/S0370157320301198 (visited on 03/02/2025).

42. Kumar, Sandeep et al. Transferable interatomic potential for aluminum from ambient conditions to warm dense matter. en. In: Physical Review Research 5.3 (Sept. 2023), p. 033162. ISSN: 2643-1564. DOI: 10.1103/PhysRevResearch.5.033162. URL: https://link.aps.org/doi/10.1103/PhysRevResearch.5.033162 (visited on 03/10/2025).

43. Thompson, A.P. et al. Spectral neighbor analysis method for automated generation of quantum-accurate interatomic potentials. en. In: Journal of Computational Physics 285 (Mar. 2015), pp. 316–330. ISSN: 00219991. DOI: 10.1016/j.jcp.2014.12.018. URL: https://linkinghub.elsevier.com/retrieve/pii/S0021999114008353 (visited on 03/21/2025).

44. "The Stopping and Range of Ions in Matter". en. In: *Treatise on Heavy-Ion Science*. Boston, MA: Springer US, 1985, pp. 93–129. ISBN: 978-1-4615-8105-5, 978-1-4615-8103-1. DOI: 10.1007/978-1-4615-8103-1_3. URL: http://link.springer.com/10.1007/978-1-4615-8103-1_3 (visited on 07/21/2025).

45. Kumar, Sandeep et al. *Training scripts and input data sets: Transferable Interatomic Potential for Aluminum from Ambient Conditions to Warm Dense Matter*. July 2023. DOI: 10.14278/RODARE.2368. URL: https://rodare.hzdr.de/record/2368 (visited on 03/21/2025).

46. Belonoshko, A. B., Ahuja, R., and Johansson, B. Quasi– *Ab Initio* Molecular Dynamic Study of Fe Melting. In: Physical Review Letters 84.16 (Apr. 2000), pp. 3638–3641. ISSN: 0031-9007, 1079-7114. DOI: 10.1103/PhysRevLett.84.3638. URL: https://link.aps.org/doi/10.1103/PhysRevLett.84.3638 (visited on 10/16/2025).

47. Plimpton, Steve. Fast Parallel Algorithms for Short-Range Molecular Dynamics. In: Journal of Computational Physics 117.1 (Mar. 1995), pp. 1–19. ISSN: 0021-9991. DOI: 10.1006/jcph.1995.1039. URL: https://www.sciencedirect.com/science/article/pii/S002199918571039X (visited on 03/10/2025).

48. Hansen, Jean-Pierre and McDonald, Ian Ranald. *Theory of simple liquids: with applications to soft matter*. Academic press, 2013.

49. Dudalov, D. E. et al. How dimensionality changes the anomalous behavior and melting scenario of a core-softened potential system? en. In: Soft Matter 10.27 (2014), pp. 4966–4976. ISSN: 1744-683X, 1744-6848. DOI: 10.1039/C4SM00124A. URL: https://xlink.rsc.org/?DOI=C4SM00124A (visited on 04/05/2025).

50. Mermin, N. D. and Wagner, H. Absence of Ferromagnetism or Antiferromagnetism in One- or Two-Dimensional Isotropic Heisenberg Models. en. In: Physical Review Letters 17.22 (Nov. 1966). Publisher: American Physical Society

(APS), pp. 1133–1136. ISSN: 0031-9007. DOI: 10.1103/physrevlett.17.1133. URL: https://link.aps.org/doi/10.1103/PhysRevLett.17.1133 (visited on 07/23/2025).